Will Nonlinear Peculiar Velocity and Inhomogeneous Reionization Spoil 21cm Cosmology from the Epoch of Reionization?

Paul R. Shapiro,[1,*] Yi Mao,[1,2,†] Ilian T. Iliev,[3] Garrelt Mellema,[4] Kanan K. Datta,[4] Kyungjin Ahn,[5] and Jun Koda[6]

[1] *Department of Astronomy and Texas Cosmology Center, University of Texas, Austin, TX 78712, USA*
[2] *UPMC Univ Paris 06, CNRS, Institut Lagrange de Paris, Institut d'Astrophysique de Paris, UMR7095, 98 bis, boulevard Arago, F-75014, Paris, France*
[3] *Astronomy Centre, Department of Physics & Astronomy, Pevensey II Building, University of Sussex, Falmer, Brighton BN1 9QH, UK*
[4] *Department of Astronomy & Oskar Klein Centre, AlbaNova, Stockholm University, SE-106 91 Stockholm, Sweden*
[5] *Department of Earth Sciences, Chosun University, Gwangju 501-759, Korea*
[6] *Centre for Astrophysics & Supercomputing, Swinburne University of Technology, Hawthorn, Victoria 3122, Australia*

(Dated: Submitted to Phys. Rev. Lett. on November 9, 2012)

The 21cm background from the epoch of reionization is a promising cosmological probe: line-of-sight velocity fluctuations distort redshift, so brightness fluctuations in Fourier space depend upon angle, which linear theory shows can separate cosmological from astrophysical information. Nonlinear fluctuations in ionization, density and velocity change this, however. The validity and accuracy of the separation scheme are tested here for the first time, by detailed reionization simulations. The scheme works reasonably well early in reionization ($\lesssim 40\%$ ionized), but not late ($\gtrsim 80\%$ ionized).

PACS numbers: 98.80.Bp,98.58.Ge,95.75.Pq

Introduction. Neutral hydrogen atoms in the intergalactic medium (IGM) at high redshift contribute a diffuse background of redshifted 21cm-line radiation which encodes a wealth of information about physical conditions in the early universe at $z > 6$, during and before the epoch of reionization (EOR). To derive *cosmological* information from this, however, we must be able to *separate* the dependence of the signal on the cosmological properties of the background universe (i.e. total matter density fluctuations) from that on the complex *astrophysical* processes that cause the thermal and ionization state of the intergalactic gas to fluctuate (e.g. energy-release from star and galaxy formation). The anisotropy introduced by the peculiar velocity of the gas, induced by structure formation, is the key to this separation.

According to linear perturbation theory, the power spectrum of the 21cm background fluctuations can be expressed as a sum of terms which depend on different powers of the cosine, $\mu_{\mathbf{k}}$, of the angle between the line-of-sight (LOS) $\mathbf{n}$ and the wavevector of a given Fourier mode $\mathbf{k}$ [1]. Different terms represent contributions from different sources of fluctuations, including fluctuations in the total matter density, velocity, and hydrogen ionized fraction, and thereby in principle provide a means of separating the effects of *cosmology* and *astrophysics*. In particular, future measurements, it is proposed [1], can be used to fit this theoretical dependence of the power spectrum on $\mu_{\mathbf{k}}$ to extract the power spectrum of total matter density fluctuations – the *cosmological* jewel.

The success of this approach, however, depends upon the validity of the linear $\mu_{\mathbf{k}}$-decomposition. While it is true that fluctuations in the total matter density at high redshift are likely to be of linear amplitude on large scales, the nonlinearity of small-scale structure in density, velocity and reionization patchiness can leave its imprint on the 21cm signal, which might result in nonlinear distortion in the 3D power spectrum of 21cm brightness temperature fluctuations and so spoil the linear $\mu_{\mathbf{k}}$-decomposition. In what follows, we will examine this question. We will assess the accuracy of this method for deriving cosmological information from the 21cm background by using the results of new large-scale N-body+radiative transfer simulations of cosmic reionization as mock data from which to "measure" the matter density power spectrum. Our simulation volume $(425\,\mathrm{Mpc}/h)^3$ is large enough to make the sampling errors smaller than the systematic errors, while approaching the size of upcoming surveys like LOFAR[2] ($5^\circ \times 5^\circ$).

The 21cm brightness temperature in redshift space. The observed frequency $\nu_{\rm obs}$ reflects both the cosmological redshift $z_{\rm cos}$ from the time of emission and the Doppler shift associated with the peculiar radial velocity $v_\parallel$ there, i.e. $\nu_{\rm obs} = \nu_0/(1+z_{\rm obs})$, where $1+z_{\rm obs} = (1+z_{\rm cos})(1-\frac{v_\parallel}{c})^{-1}$. In the "distorted" comoving coordinate system known as *redshift* space, the position of the emitter is the *apparent* comoving position if the redshift is interpreted as cosmological only, which shifts the *real* comoving coordinate $\mathbf{r}$ along the LOS to $\mathbf{s} = \mathbf{r} + \left(v_\parallel/aH(z)\right)\mathbf{n}$, where $a \equiv (1+z_{\rm cos})^{-1}$ is the cosmic scale factor. Henceforth, superscripts "r" and "s" denote quantities in real- and redshift-space, respectively, and we will write z for $z_{\rm cos}$ unless otherwise noted.

Peculiar velocity can enhance/suppress the 21cm brightness temperature measured relative to that of the cosmic microwave background (CMB), from over/under-

dense regions [1],

$$\delta T_b^s(\mathbf{s}) = \delta T_b^r(\mathbf{r}) = \widehat{\delta T}_b(z)\,\frac{1+\delta^r_{\rho_{\rm HI}}(\mathbf{r})}{\left|1+\delta^r_{\partial_r v}(\mathbf{r})\right|}\,. \qquad (1)$$

Here we focus on the limit where the spin temperature $T_s^r \gg T_{\rm CMB}$, valid soon after reionization begins. As such, we can neglect the dependence on spin temperature, but our discussion can be readily generalized to the case of finite T_s^r. In equation (1), $\widehat{\delta T}_b(z) = (23.88\,{\rm mK})\left(\frac{\Omega_{\rm b}h^2}{0.02}\right)\sqrt{\frac{0.15}{\Omega_{\rm M}h^2}\frac{1+z}{10}}\bar{x}_{\rm HI,m}(z)$ is the mean 21cm signal (where $\bar{x}_{\rm HI,m}(z)$ is the mass-weighted global neutral fraction), $\delta^r_{\rho_{\rm HI}}(\mathbf{r})$ is the neutral hydrogen overdensity, and $\delta^r_{\partial_r v}(\mathbf{r}) \equiv \frac{1+z}{H(z)}\frac{dv_\parallel}{dr_\parallel}(\mathbf{r})$ is the gradient of proper radial peculiar velocity along the LOS, normalized by $\frac{H}{1+z}$, where $H(z)$ is the Hubble parameter.

The 21cm power spectrum anisotropy in redshift-space. In Fourier space, the three-dimensional power spectrum of 21cm brightness temperature (hereafter "21cm power spectrum") is defined as $\left\langle \widetilde{\delta T_b}^*(\mathbf{k})\widetilde{\delta T_b}(\mathbf{k}')\right\rangle \equiv (2\pi)^3 P_{\Delta T}(\mathbf{k})\delta^{(3)}(\mathbf{k}-\mathbf{k}')$. There are three approaches to model the 21cm signal in redshift space, based on different assumptions on peculiar velocity and reionization patchiness, as follows.

• *Linear scheme (linear velocity-density relation, linearized neutral fraction fluctuations).* As described above, the linear scheme was originally proposed in the context of linear perturbation theory [1] and later rederived with weaker assumptions [3] which are: (1) the velocity ($\mathbf{v}^r$) and total density fluctuations (δ^r_ρ) satisfy the linear relation, $\widetilde{v^r_\parallel}(\mathbf{k}) = i\left(\frac{H(z)}{1+z}\right)\widetilde{\delta^r_\rho}(\mathbf{k})\mu_{\mathbf{k}}/k$, (2) the baryon distribution traces the CDM, (3) the peculiar velocity, the hydrogen density fluctuation ($\delta^r_{\rho_{\rm H}}$), and the *neutral fraction* fluctuation ($\delta^r_{x_{\rm HI}}$) are all linearized. Under these assumptions, the 3D 21cm power spectrum can be expanded in polynomials of $\mu_{\mathbf{k}} \equiv \mathbf{k}\cdot\mathbf{n}/|\mathbf{k}|$,

$$P^{s,\rm lin}_{\Delta T}(\mathbf{k},z) = P_{\mu^0}(k,z) + P_{\mu^2}(k,z)\mu^2_{\mathbf{k}} + P_{\mu^4}(k,z)\mu^4_{\mathbf{k}}\,, \quad (2)$$

where the moments $\{P_{\mu^0}, P_{\mu^2}, P_{\mu^4}\}$ are functions of only $k = |\mathbf{k}|$ and redshift z. More importantly, the 4$^{\rm th}$-moment depends only on the total density power spectrum $P^{r,\rm total}_{\delta_\rho,\delta_\rho}$ and the global neutral fraction $\bar{x}_{\rm HI,m}(z)$,

$$P_{\mu^4}(k,z) = \widehat{\delta T}_b^2(z) P^{r,\rm total}_{\delta_\rho,\delta_\rho}(k,z)\,, \qquad (3)$$

while other moments are "contaminated" by power spectra due to reionization and/or spin temperature. In principle, then, cosmological information can be extracted from the 21cm signal by fitting the measured $P^s_{\Delta T}(\mathbf{k},z)$ to equation (2) to isolate the 4$^{\rm th}$ moment.

• *Quasi-linear $\mu_{\mathbf{k}}$-decomposition scheme (linear velocity-density relation, linearized neutral overdensity).* The assumption of $\delta^r_{x_{\rm HI}} \ll 1$ breaks down when $\bar{x}_{\rm HI,m} > 0.5$, which results in a significant contribution to the power spectrum from higher-order terms, e.g. $P^r_{\delta_{x_{\rm HI}}\delta_{\rho_{\rm H}},\delta_{x_{\rm HI}}}$ [4], etc. Fortunately, the 3D 21cm power spectrum can still be written in the form of equation (2), and, more importantly, the 4$^{\rm th}$-moment is still related to the matter power spectrum as in equation (3), if we adopt the same assumptions (1) and (2) as in the linear scheme, but assume peculiar velocity and the *neutral density* fluctuation $\delta^r_{\rho_{\rm HI}} = \delta^r_{\rho_{\rm H}} + \delta^r_{x_{\rm HI}} + \delta^r_{\rho_{\rm H}}\delta^r_{x_{\rm HI}}$, as opposed to $\delta^r_{x_{\rm HI}}$ alone, are linearized. This is the so-called quasi-linear $\mu_{\mathbf{k}}$-decomposition formalism [3], in which only lower moments differ from the linear scheme prediction.

• *Fully-nonlinear scheme (nonlinear velocity, nonlinear neutral overdensity).* In the optically-thin approximation, two nonlinear effects of peculiar velocity must be taken into account: (1) the 21cm brightness temperature is corrected for velocity gradient as in equation (1); (2) when the *real*-space comoving coordinates $\mathbf{r}$ are mapped to *redshift*-space coordinates, volume elements are also resized according to $\delta V^s(\mathbf{s}) = \delta V^r(\mathbf{r})\left|1+\delta^r_{\partial_r v}(\mathbf{r})\right|$. Fortunately, the combined effect allows us to compute the 21cm brightness temperature in redshift-space with a simple formula [3]

$$\delta T_b^s(\mathbf{s}) = \widehat{\delta T}_b(z)\,\left[1+\delta^s_{\rho_{\rm HI}}(\mathbf{s})\right]\,, \qquad (4)$$

where $\delta^s_{\rho_{\rm HI}}(\mathbf{s}) = n^s_{\rm HI}(\mathbf{s})/\bar{n}_{\rm HI}(z) - 1$ is the neutral overdensity in redshift-space.

Angular separation of 3D power spectrum. Given the observed 3D power spectrum on a uniform 3D grid in $\mathbf{k}$-space, its moments can be decomposed using the χ^2-fit as follows. For a given LOS, 3D modes $P^s_{\Delta T}(\mathbf{k})$ with the same $\mu_{\mathbf{k}}$ and same k but different azimuthal angle are averaged to give a measure of $\overline{P^s_{\Delta T}}(k,\mu_{\mathbf{k}})$ and the associated sampling variance $\sigma^2_P(k,\mu_{\mathbf{k}}) = (2/N_{\mu_{\mathbf{k}},k})\,\overline{P^s_{\Delta T}}^2(k,\mu_{\mathbf{k}})$, where $N_{\mu_{\mathbf{k}},k}$ is the number of modes with the same $\mu_{\mathbf{k}}$ and k. For the 3D grid from the simulated data described below, we further combine the measures along three different LOS, tripling the number of modes. Next, modes are grouped in spherical k-shells with the width $\Delta k/k = 0.186$ (chosen as a trade-off between minimal mean χ^2 and minimal numerical noise, but our results below are insensitive to this value). For each shell (the k-dependence is implicit below), we shall fit the data set $\left\{\mu_i, \overline{P^s_{\Delta T}}(\mu_i), \sigma_P(\mu_i)\right\}$ (where i runs through all modes within the shell) with the ansatz $P^s_{\Delta T}(\mu) = \sum_{j=1}^3 a_j X_j(\mu)$, where basis functions $X_j(\mu) = \{1,\mu^2,\mu^4\}$ and coefficients $a_j = \{P_{\mu^0}, P_{\mu^2}, P_{\mu^4}\}$, for $j = 1,2,3$, respectively. To minimize the merit function $\chi^2 = \sum_i\left[\left(\overline{P^s_{\Delta T}}(\mu_i) - \sum_{j=1}^3 a_j X_j(\mu_i)\right)/\sigma_P(\mu_i)\right]^2$, we employ the standard General Linear Least Squares method (see, e.g. [5]). This results in best-fit coefficients $a_j = \sum_{k=1}^3 C_{jk}\,\beta_k$ with associated error esti-

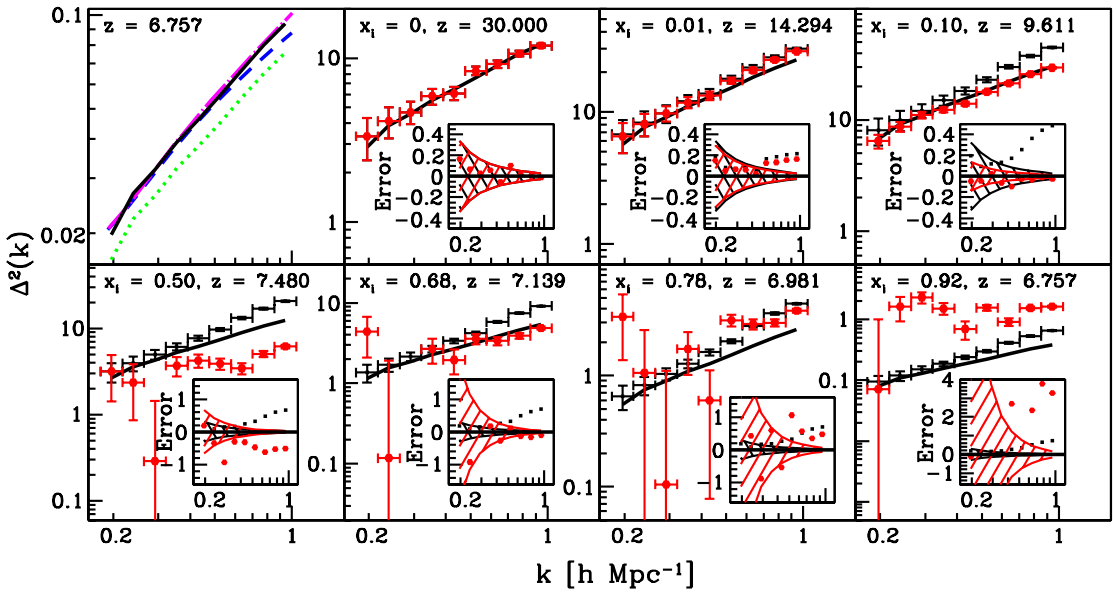

FIG. 1. Top left panel: the angle-averaged matter density power spectrum, $\Delta^2_{\delta\delta} = k^3 P_{\delta\delta}(k)/2\pi^2$ (unitless), from N-body results for *total* matter (solid/black) and for *IGM* matter (green/dot), linear total density (dashed/blue), and 3PT total density (dot-dashed/magenta), at $z = 6.757$. Other panels: the total matter density power spectrum (multiplied by $\widehat{\delta T_b}^2(z)$, the square of mean 21cm brightness temperature) as "measured" by fitting the mock data (i.e. reionization simulation) for the 3D power spectrum of 21cm brightness temperature anisotropy to the $\mu_{\mathbf{k}}$-decomposition, $\Delta^2_{\mu^4} = k^3 P_{\mu^4}(k)/2\pi^2$ (in mK^2), at different phases of reionization (mass-weighted global ionization fraction $\bar{x}_{i,m} = 0$, 0.01, 0.10, 0.50, 0.68, 0.78, and 0.92, respectively). Red data points are reionization simulation results. Black data points assume homogeneously-ionized IGM with same global mean $\bar{x}_{i,m}$ as reionization simulation. Solid black curves are the expectation from linear scheme, i.e. equation (3) evaluated using *total* density power spectra from N-body simulation (multiplied by $\widehat{\delta T_b}^2(z)$). Fractional errors plotted in inset are with respect to the linear expectation, i.e. $(P^{\rm best-fit}_{\mu^4} - P^{\rm linear}_{\mu^4})/P^{\rm linear}_{\mu^4}$. Error bars and shaded regions correspond to the sampling variance of the simulation volume.

mates $\sigma(a_j) = \sqrt{C_{jj}}$. Here we define the 3×3 matrix $\alpha_{jk} = \sum_i X_j(\mu_i) X_k(\mu_i)/\sigma_P^2(\mu_i)$, whose inverse is the covariance matrix $C = \alpha^{-1}$, and a 3-vector $\beta_j = \sum_i \overline{P^s_{\Delta T}}(\mu_i) X_j(\mu_i)/\sigma_P^2(\mu_i)$.

Mock data from a reionization simulation. We perform a new large-scale, high-resolution N-body simulation of the ΛCDM universe (performed with the CubeP^{3}M code [6, 7]) in a comoving volume of $L_{\rm box} = 425\,{\rm Mpc}/h$ on each side using 5488^3 (165 billion) particles. To find halos, we use the spherical overdensity method and require them to consist of at least 20 N-body particles; this implies a minimum halo mass of $10^9\,M_\odot$. We use subgrid modeling to compute the halo population with mass between $10^8 - 10^9\,M_\odot$. Assuming that the gas traces the CDM particles exactly, we grid the density and velocity in the IGM (i.e. halo mass excluded) on a 504^3 grid using SPH-like smoothing with an adaptive kernel. Halo lists and density fields are then processed with the radiative transfer code C^{2}Ray [8]. Each halo releases f_γ ionizing photons per baryon per $\Delta t = 11.5\,{\rm Myrs}$, with $f_\gamma = 10$ ($f_\gamma = 2$) for halos below $10^9\,M_\odot$ (above $10^9\,M_\odot$), respectively. To incorporate feedback from reionization, halos less massive than $10^9\,M_\odot$ located in ionized regions do not produce any photons. We refer the readers to [9] for the elaboration of the codes and the feedback process, and Iliev et al. (*in prep.*) for the details of this simulation. The simulation used the following set of cosmological parameters $\Omega_\Lambda = 0.73, \Omega_{\rm M} = 0.27, \Omega_{\rm b} = 0.044, h = 0.7, \sigma_8 = 0.8, n_{\rm s} = 0.96$ where $H_0 = 100h\,{\rm km\,s^{-1}\,Mpc^{-1}}$, consistent with the *WMAP* seven-year results [10].

We then use the nonlinear density, velocity and ionization data from the simulation to calculate the nonlinear 3D 21cm power spectrum, using the MM-RRM scheme in [3] for mapping N-body and reionization grid data in real space onto a redshift-space grid, and separate out the best-fit 4$^{\rm th}$-moment using the aforementioned angular separation prescription. The linear and quasi-linear schemes both predict that this 4$^{\rm th}$-moment should be given by equation (3), which we test by evaluating the r.h.s. of equation (3) directly from the simulation N-body results, for comparison. Some preliminary results were previously summarized by us in [11].

Results and discussions. In Figure 1, we plot the best-fit 4$^{\rm th}$-moment of the fully nonlinear power spectrum, and the benchmark linear expectation (i.e. equation (3) evaluated with nonlinear simulation data). Note

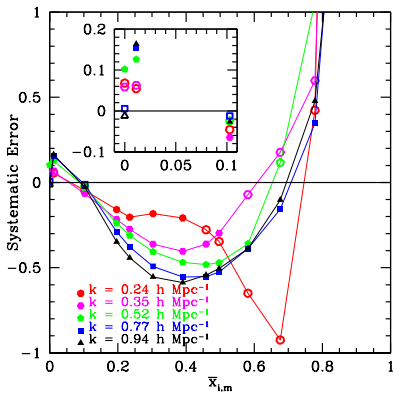

FIG. 2. Systematic error of the separation scheme. We plot the fractional error of the best-fit $4^{\rm th}$-moment with respect to the linear expectation, in the inhomogeneous reionization case, as a function of global ionization fraction $\bar{x}_{i,m}$, for $k = 0.24, 0.35, 0.52, 0.77, 0.94\,h\,{\rm Mpc}^{-1}$, respectively. The solid/open dots correspond to the case where the systematic error is greater/less than the sampling error of our simulation. The inset is zoom-in to $0 \leq \bar{x}_{i,m} \leq 0.10$.

that, while the mock 21cm signal is from the IGM, as is the observed signal, the *total* density power spectrum is expected in the linear scheme. (There is a difference between the *total* and *IGM* density power spectra, as in Figure 1, resulting from the exclusion of particle mass in halos when computing the IGM density.) We focus on the range of wavenumbers, $0.2 < k < 1\,h\,{\rm Mpc}^{-1}$, for which k is large enough to avoid a large sampling variance but small enough to avoid a large aliasing effect.

• *Consistency check of the decomposition pipeline.* We confirm that: (1) the total density power spectrum from N-body simulation agrees with the linear power spectrum (from CAMB[12]) at large scales $k \lesssim 0.5\,h\,{\rm Mpc}^{-1}$. At smaller scales, it agrees with the result from third-order perturbation theory (3PT)[13], but is enhanced relative to the linear power spectrum. (2) The best-fit $4^{\rm th}$-moment agrees with the total density power spectrum at $z = 30$ when the IGM is everywhere neutral and the density fluctuations are of linear amplitude.

• *Effect of IGM nonlinear density/velocity fluctuations.* For diagnostic purposes, we first investigate the case in which the ionized fraction at each point in the IGM is set equal to the (mass-weighted) global mean value $\bar{x}_{i,m}$ in the reionization simulation at that redshift. In this case, the best-fit $4^{\rm th}$-moment at different redshifts is enhanced with respect to the total density power spectrum, and the deviation increases from 20% ($z \simeq 14$) to 70% ($z \simeq 7$), as structure formation proceeds. These results show that nonlinear density and velocity fluctuations cause the $\mu_{\mathbf{k}}$-decomposition to make a systematic error, not caused by ionization patchiness.

• *Effect of inhomogeneous reionization and nonlinear velocity fluctuations.* Early in reionization, the best-fit $4^{\rm th}$-moment for inhomogeneous reionization is suppressed relative to that for the homogeneously partially-ionized case. This is because fluctuations in neutral fraction and density anticorrelate in a universe reionized "inside-out," i.e. overdense regions are ionized earlier on average than underdense regions. More precisely, inhomogeneous reionization affects the anisotropy through its coupling with nonlinear velocity fluctuations, because reionization patchiness, alone, cannot introduce anisotropy in 21cm power spectrum (e.g. in the quasi-linear $\mu_{\mathbf{k}}$-decomposition scheme). A quantitative explanation will be formulated in more detail in Mao et al. (*in prep.*).

This effect cancels the enhancement due to nonlinear fluctuations in IGM density and velocity, alone. Incidentally, the systematic error (i.e. departure of the best-fit $4^{\rm th}$-moment from linear expectation) first crosses zero (less than 10% at all scales) when $\bar{x}_{i,m} \approx 10\%$ ($z \simeq 9.6$ in our simulation). Afterwards, this error grows to 60% for $\bar{x}_{i,m} \lesssim 50\%$. As determined by the competition between these two effects, this error depends on both the reionization epoch and the scale of interest — the smaller the ionized fraction $\bar{x}_{i,m}$ and the smaller the wavenumber k, the smaller the error (see Figure 2).

As the typical size of ionized regions grows larger than the scales plotted here, the best-fit $4^{\rm th}$-moment at $k = 0.5 - 1\,h\,{\rm Mpc}^{-1}$ becomes less suppressed after the 50% ionized epoch. For *this* k-range, the net error changes sign again when $\bar{x}_{i,m} \simeq 68\%$ (with error $< 20\%$).

At late epochs ($\bar{x}_{i,m} \gtrsim 0.8$, $z \lesssim 7$), the systematic error for all scales is large, $\gtrsim 100\%$. This is due to the breakdown of the perturbative expansion, i.e. the expansion of the 3D 21cm power spectrum in neutral density fluctuations becomes divergent when $\delta_{\rho_{\rm HI}} \gtrsim \mathcal{O}(1)$, as the ionized bubbles expand and percolate in the universe. In addition, the lightcone effect[14] becomes non-negligible at this late time, and can further squeeze the anisotropic power spectrum along the LOS, as does the redshift-space distortion. Therefore, the estimate of 100% error here is only a lower limit to the actual error at late times.

• *The sampling variance.* Our simulation volume is large enough that these systematic errors quoted above are all greater than the estimated sampling errors (except when the systematic error crosses zero), so they represent statistically significant deviations from the expectations of the $\mu_{\mathbf{k}}$-decomposition, rather than accidents of the particular numerical realization.

Conclusion. This *letter* is the first attempt to quantify in detail the *intrinsic* precision of the linear scheme in which the cosmological matter density power spectrum can be extracted from 21cm observations of the EOR. Two effects may spoil the extraction, a major one due to the coupling between inhomogeneous reionization and nonlinear velocity, and a minor one due to nonlinear density and velocity fluctuations alone. The competition

between these identifies two phases of reionization particularly interesting to cosmology — $\bar{x}_{i,m} \simeq 68\%$, where systematic error is within 20% for $k = 0.5 - 1\,h\,\mathrm{Mpc}^{-1}$, and $\bar{x}_{i,m} \simeq 10\%$, where systematic error is within 10% for *all* wavenumbers. The epoch of exact crossover is likely to depend on the reionization scenario, as does the reionization patchiness. The 68%-ionized epoch is more accessible to first-generation observations (e.g. LOFAR, MWA[15]) because of smaller foreground and thermal noise at lower redshift.

We summarize our results in Figure 2. We see that, for ionized fraction less than 40% ($z \simeq 7.760$), the linear $\mu_{\mathbf{k}}$-decomposition works well for large-scale measurement $k \lesssim 0.24\,h\,\mathrm{Mpc}^{-1}$, with errors within 20%, and its application could still be acceptable at smaller scales, down to $k \simeq 0.5\,h\,\mathrm{Mpc}^{-1}$, with errors up to 50%. During the intermediate phase of reionization ($\bar{x}_{i,m} \simeq 0.4 - 0.7$), decomposition at the intermediate k-range, $k \simeq 0.35 - 0.5\,h\,\mathrm{Mpc}^{-1}$, is acceptable with errors up to 50%. However, in the late stage of reionization ($\bar{x}_{i,m} \gtrsim 0.8$), it is difficult to use 21cm measurement to extract the cosmological information in the approach proposed by the linear scheme, because the systematic error is of order unity. Measurements at very large scale $k < 0.2\,h\,\mathrm{Mpc}^{-1}$ might still be useful at this late phase, but a survey volume much larger than that of LOFAR (which is comparable to our simulation volume) is necessary to reduce the sampling variance in the 4^{th}-moment significantly (e.g. MWA with 30° field of view).

Acknowledgements: This work was supported in part by NSF grants AST-0708176 and AST-1009799, NASA grants NNX07AH09G, NNG04G177G and NNX11AE09G, Chandra grant SAO TM8-9009X, the French state funds managed by the ANR within the Investissements d'Avenir programme under reference ANR-11-IDEX-0004-02, the Science and Technology Facilities Council [grant numbers ST/F002858/1 and ST/I000976/1], and the Southeast Physics Network (SEPNet). The authors acknowledge the Texas Advanced Computing Center (TACC) and the National Institute for Computational Sciences (NICS) for providing HPC resources, under NSF TeraGrid grants TG-AST0900005 and TG-080028N and TACC internal allocation grant "A-asoz". Computations were performed on the GPC supercomputer at the SciNet HPC Consortium. SciNet is funded by: the Canada Foundation for Innovation under the auspices of Compute Canada; the Government of Ontario; Ontario Research Fund - Research Excellence; and the University of Toronto.

* shapiro@astro.as.utexas.edu (PRS)
† mao@iap.fr (YM)

[1] R. Barkana and A. Loeb, ApJL, **624**, L65 (2005)
[2] `http://www.lofar.org`; see, also, van Haarlem et al.(*in prep.*).
[3] Y. Mao, P. R. Shapiro, G. Mellema, I. T. Iliev, J. Koda, & K. Ahn, MNRAS, **422**, 926 (2012)
[4] A. Lidz, O. Zahn, M. McQuinn, M. Zaldarriaga, & S. Dutta, ApJ, **659**, 865 (2007)
[5] W. H. Press, S. A. Teukolsky, W. T. Vetterling, & B. P. Flannery, Numerical Recipes: The Art of Scientific Computing (3rd ed.), Cambridge University Press, pp.665-668 (2007)
[6] I. T. Iliev, P. R. Shapiro, G. Mellema, H. Merz, and U.-L. Pen, Proceedings of the TeraGrid 2008 Conference, p.31, (ArXiv:0806.2887) (2008)
[7] J. Harnois-Deraps, U.-L. Pen, I. T. Iliev, H. Merz, J. D. Emberson, and V. Desjacques, MNRAS, submitted, (ArXiv:1208.5098) (2012)
[8] G. Mellema, I. T. Iliev, M. A. Alvarez, and P. R. Shapiro, New Astronomy, **11**, 374 (2006)
[9] I. T. Iliev, G. Mellema, P. R. Shapiro, U.-L. Pen, Y. Mao, J. Koda, & K. Ahn, MNRAS, **423**, 2222 (2012)
[10] E. Komatsu, et al. [WMAP Collaboration], ApJS, **192**, 18 (2011)
[11] Mao, Y., Shapiro, P. R., Iliev, I. T., Mellema, G., Koda, J., & Pen, U.-L., ASP Conference Series Vol. **432**, 212 (2010)
[12] A. Lewis and S. Bridle, Phys. Rev., **D66**, 103511 (2002); see also `http://camb.info/`.
[13] D. Jeong and E. Komatsu, ApJ, **651**, 619 (2006)
[14] K. K. Datta, G. Mellema, Y. Mao, I. T. Iliev, P. R. Shapiro, and K. Ahn, MNRAS, **424**, 1877 (2012)
[15] S. J. Tingay, et al. [MWA Collaboration], PASA, submitted (ArXiv:1206.6945) (2012); see also `http://www.mwatelescope.org/`.